

Comparison of two techniques for estimation of thermal diffusivity with MRgHIFU

Christopher Reed Dillon¹, Allison Payne², and Robert Roemer³

¹Bioengineering, University of Utah, Salt Lake City, UT, United States, ²Utah Center for Advanced Imaging Research, University of Utah, Salt Lake City, UT, United States, ³Mechanical Engineering, University of Utah, Salt Lake City, UT, United States

Target audience: Medical physicists interested in patient-specific tissue thermal properties for thermal therapies.

Purpose: Because of large spatial temperature gradients induced by magnetic resonance-guided high intensity focused ultrasound (MRgHIFU), conduction plays a significant role in HIFU treatments and their outcomes. High variability in published property tables for thermal diffusivity demonstrates the necessity of patient-specific thermal property determination. This study will compare two methods for using MRgHIFU at non-ablative levels to estimate thermal diffusivity.

Theory: Each estimation technique fits the transverse MRgHIFU temperature data (see Figure 1) to an appropriate analytical temperature solution. The first technique uses a solution wherein the ultrasonic power deposition pattern is approximated by a 1-D radial (r or xy) Gaussian. The solution assumes that axial conduction and all perfusion effects are negligible.¹ The heating solution from Dillon² is $T_{Heat}(r, t) = C \left(\frac{\beta}{4\kappa} \right) \left[Ei \left(\frac{-r^2}{\beta} \right) - Ei \left(\frac{-r^2}{\beta(1+4\kappa t/\beta)} \right) \right]$, (1) where C is the initial slope of temperature rise on the beam axis, β is the ultrasound Gaussian variance, and κ is the thermal diffusivity. By applying the principle of superposition, the temperature distribution after the ultrasound is turned off is given by:

$$T_{Cool}(r, t) = C \left(\frac{\beta}{4\kappa} \right) \left[-Ei \left(\frac{-r^2}{\beta(1+4\kappa t/\beta)} \right) + Ei \left(\frac{-r^2}{\beta(1+4\kappa(t-t_{off})/\beta)} \right) \right]. \quad (2)$$

When the radial distance r , heating duration t_{off} , and time t since the onset of heating are known, a least-squares three parameter fit to the temperature data using Eq. 1 during heating and Eq. 2 during cooling is possible. The estimate for the tissue thermal diffusivity is found directly from fitting parameter κ .

The second estimation technique, first proposed by Cheng and Plewes³, also assumes a 1-D radial Gaussian pattern which neglects axial conduction. In their analytical solution, however, all heating is induced with an instantaneous pulse. The analytical cooling solution for this case can be simplified as $T_{Cool}(r, t) = A \cdot \exp \left[-\frac{r^2}{4\kappa(t+r_0^2/2\kappa)} \right]$, (3) where A is the time- and perfusion-dependent temperature on the beam axis and r_0 is the

initial Gaussian radius of the beam. The rate at which this Gaussian function expands equals 4κ . Thus, by measuring the beam width of the decaying temperatures over time, an estimate of the thermal diffusivity can be made.

Methods: SAR patterns were modeled for a 256-element phased array transducer (Imasonics) using the hybrid angular spectrum method.⁴ For each simulated SAR pattern, the bioheat transfer equation⁵ was used to generate temperature data for 60 total seconds. The ultrasound heating time was varied from 1 to 40 seconds and power was adjusted to reach a maximum focal temperature of 10°C. Estimates of thermal diffusivity were made with each estimation technique. These data were replicated experimentally in ex vivo pork loin. MR temperatures were acquired with a 3T Siemens Trio MRI [3D seg-EPI, TR/TE=35/11 ms, FA=15°, 766 Hz/pixel, EPI factor=9, 1x1x3 mm³, 4.2 s]. Temperature data was zero filled interpolated to 0.5-mm isotropic resolution prior to thermal diffusivity estimation.

Results: Figure 2 shows diffusivity errors for simulated heating times ranging from 1 to 40 seconds. Figure 3 shows experimental results in ex vivo pork loin ($n=4$) for 42 s of heating and 63 s total data. Error bars extend to ± 1 standard deviation from the mean of diffusivity estimates. Figure 4a shows the experimental temperatures at the end of heating in a 2x2 cm² region at the focal zone. Figure 4b shows the fitted temperature profile from Eq. 1 for the same time and region. Figure 4c is the difference between the fitted and experimental temperatures with a maximum of 1.1°C.

Discussion and Conclusions: Simulation results suggest that the Dillon technique is consistently more accurate than the Cheng and Plewes method. Both methods estimate pork loin thermal diffusivity within the range of published values, though the Cheng and Plewes method had greater variability in its estimations. Each method has potential to improve patient treatment planning of MRgHIFU treatments.

Acknowledgments: The authors gratefully acknowledge support from Siemens Healthcare AG, the FUS Foundation, the Ben and Iris Margolis Foundation, and NIH grants R01 CA87785, R01 CA134599, and R01 EB013433.

References:

- 1) Parker K. J Acoust Soc Am. 1985;77:719-25.
- 2) Dillon C, et al. Phys Med Biol. 2012;57:4527-4544.
- 3) Cheng H and Plewes D. J Magn Reson Imaging. 2002;16:598-609.
- 4) Vyas U and Christensen D. IEEE Trans Ultrason Ferroelectr Freq Control. 2012;59:1093-1100.
- 5) Pennes H. J Appl Physiol. 1948;1:93-122.

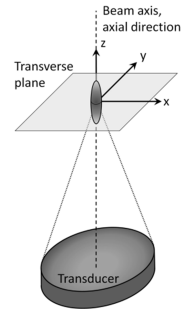


Figure 1: Schematic of simulation and experimental setup.

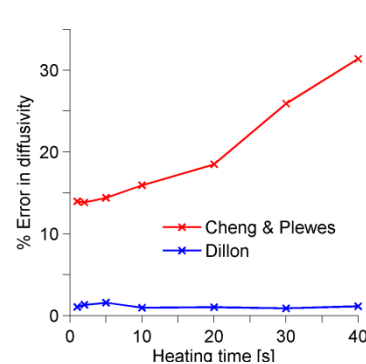


Figure 2: Diffusivity estimation results for simulations with varied heating times.

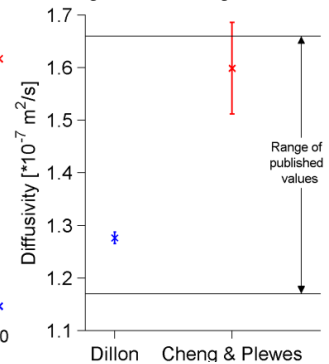


Figure 3: Experimental diffusivity estimates in ex vivo pork loin ($n=4$). 42 s heating, 63 s total data.

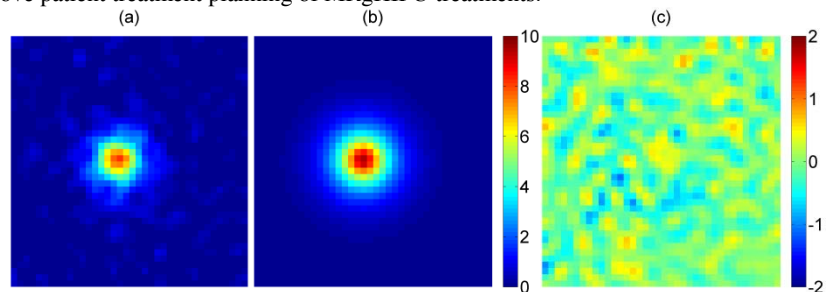


Figure 4: (a) Experimental temperatures in a 2x2 cm² region at the end of heating, (b) Fitted temperatures from Eq. 1, (c) Difference between fitted and experimental temperatures.